https://doi.org/10.1016/j.apenergy.2017.08.169

Recycled waste black polyurethane sponges for solar vapor generation and distillation

Sainan Ma[1], Chun Pang Chiu[1], Yujiao Zhu[1], Chun Yin Tang[1,2], Hui Long[1,2], Wayesh Qarony[1], Xinhua Zhao[1], Xuming Zhang[1], Wai Hung Lo[3], Yuen Hong Tsang[1,2*]

[1] Department of Applied Physics and Materials Research Center, The Hong Kong Polytechnic University, Hung Hom, Kowloon, Hong Kong, People's Republic of China

[2] The Hong Kong Polytechnic University Shenzhen Research Institute, Shenzhen, People's Republic of China

[3] Department of Applied Biology and Chemical Technology and State Key Laboratory of Chinese Medicine and Molecular Pharmacology, The Hong Kong Polytechnic University, Hung Hom, Kowloon, Hong Kong, PR China

* E-mail: yuen.tsang@polyu.edu.hk

Abstract

The abundant waste polyurethane sponge, commonly considered as one of the municipal wastes, can be recycled and converted into the valuable resources of environment. The increasing landfill cost and air-pollutions have made it a great urgent to develop the effective applications of waste polyurethane sponge. Recently, solar vapor generation has attracted extensive attentions, since energy shortage and water scarcity along with water pollution are becoming alarming global issues to be addressed. The solar vapor generation relies on the performance of the solar absorbers which convert the solar energy into heat for the vaporization process. A low cost,

efficient and durable solar absorber is vital for the development of solar vapor generation. Here, we report that the recycled self-floating black polyurethane sponges are very promising solar absorber materials. which can efficiently generate water vapor after a simple one-step hydrophilic treatment with dopamine hydrochloride. The evaporating rate was more than 3.5 times higher compared to that of the existing natural evaporation process, exhibiting an evaporation efficiency of above 50%. Furthermore, this black polyurethane sponge can also drive solar ethanol distillation, yielding up to 25 wt% concentration promotion under each distillation cycle.

Keywords: Solar vapor generation, heat localization, black sponge, recycled, hydrophilic, solar distillation

1. Introduction

Given the increasing global concerns of energy problems, renewable energy resources have been pursued in high demand, among which solar power is the most promising and naturally unlimited energy source in the foreseeable future. The solar energy that reaches the earth in an hour is able to cover the energy consumption of human for an entire year [1]. Practical technologies should be developed for better utilization of the solar energy for the energy consumption of human [2]. At present, solar thermal conversion technology comes to be the most effective one compared with other solar energy utilization approaches such as photocatalysis or photovoltaics [3-5]. Traditional vaporization is expensive and usually involves the consumption of depletable fossil fuels with heavy emissions of greenhouse gas, e.g. CO_2 [6, 7]. Recently, the utilization of solar energy to enhance evaporation emerges to be an attractive strategy for

sustainable and practical systems, which shows great potential applications in sterilizations [8], wastewater treatment [9, 10], desalination [11-13] and ethanol distillation [14, 15]. The solar evaporation relies on the development of a key component, *i.e.* solar absorber, which converts the solar energy into heat to vaporize water. The research on solar absorber materials is the main approach to realize the practical use of the solar evaporation technology.

In recent years, the plasmonic metallic nanoparticles have been most widely investigated as the solar absorbers due to their unique photothermal conversion property. Halas's group firstly introduced that the suspended gold nanoparticles can generate vapour bubbles for efficient evaporations of surrounding liquid because of their high solar absorption and scattering properties [14, 16]. However, these methods usually require costly high optical concentrations (up to 10^3 kW m^{-2}), and only a relatively low solar-thermal efficiency of about 24% has been obtained. As the heat is generated around the nanoparticles, large amount of the thermal energy will be transferred to heat up the surrounding liquid during the vapour bubbles rising to the evaporative surface. To overcome this problem, the plasmonic films were further demonstrated as high-performance and broadband absorbers to localize plasmonic heat at the air-water interface [17-21]. An efficiency of ~85% under the irradiation density of 10 kW m^{-2} was achieved by bio-inspired solar steam generation using floating Au nanoparticles membranes [22]. However, except that the focusing optics are usually required, the scarcity and high cost of metallic absorbers involving noble metals limit their practical applications. Moreover, after the long-time illumination, the plasmonic nanoparticles may fuse together and the plasmonic properties can be weakened, which results in lower solar thermal conversion efficiency [23].

Recently, more common non-metallic materials, such as carbon black [24, 25], carbon nanotube [26], graphene and graphene oxide [27, 28], polypyrrole (ppy) coated mesh [29], and

bio-inspired materials like wood and mushrooms [30-32], have been extensively investigated for solar vapor generation with higher operation stability and lower cost compared with plasmonic metallic materials. Among these absorbers, bilayer structures are often proposed for the efficient solar evaporation with the top layer of photothermal materials for light absorption and heat conversion, and the bottom layer of thermal insulating materials with low thermal conductivity to prevent the heat loss [33-36]. Highly efficient solar vapor generation was achieved based on the carbon black coated paper supported by expanded polystyrene foam with a thermal efficiency of 88% under one sun irradiation [25]. These studies have been devoted to study the solar absorbers for high solar-thermal efficiency, which usually possess the unique features for the improvement of solar thermal conversion efficiency such as low material density so that it will float on the water surface, low thermal conductivity to reduce heat loss, hydrophilic and porous structure for fast fluid transport. However, these proposed absorbers usually have their own limitations, which are either not common, carbonation needed or too expensive for the practical application. Recycling and reutilizing is currently the trend for developing sustainable society. Using some common wastes as the absorbers for solar evaporation can be a new and popular research direction to reduce the overall cost and energy consumption for production, which ultimately achieves the goal of green energy and sustainable development.

Black polyurethane (BPU) sponge, one kind of three dimensional porous materials, has been widely used as anti-seismic packaging materials for transportation in our daily life today. The production of black PU sponges as packaging material comes to millions of tons every year [37-39]. However, most of them are abandoned after one-time utilization and cannot easily decompose naturally [40]. More and more attention is being paid on the recycling of PU sponge with the rise of regulatory and environmental issues. People are focusing on seeking alternative

options to dispose these polyurethane materials for the conservation of petroleum resources and the reduction of environmental stress [41]. Recently, researchers have applied the PU sponges in areas such as reusable oil-absorbent [42, 43] and templates for constructing porous structures [44, 45].

In this work, for the first time we demonstrate that the recycled black PU sponge with porous structure, low thermal conductivity (~0.034 W/mK) [46], and low mass density to be self-floating, could behave as an ideal absorber for solar vapor generation except for its weak hydrophilicity. Therefore, surface chemical properties were modified by a facile dopamine solution stirring treatment to achieve the fast dynamic wettability of the BPU sponges for fluent water supply on the top surface of the absorber. The surface modified PU (SM-BPU) sponge showed that the evaporating rate increased more than 3.5 times compared to the existing natural evaporation process. The BPU sponge for solar ethanol distillation application was further examined and the results showed that this sponge can yield up to 25 wt% concentration promotion under each distillation cycle. Considering the BPU sponge as the major waste of packaging industry, the recycling of the waste BPU sponge for solar energy conversion can reduce the environmental pressure. While in conventional evaporation systems, it needs the consumption of fossil energy, which is a limited energy resource and generates greenhouse gas and pollutants during the combustion. From the views of environmental sustainability and energy cost, this work promises to be attractive and competitive for applications in practical solar-thermal technologies.

2. Material and methods

2.1. Material.

The black polyurethane (BPU) sponge with a pore diameter of ~300 μm, density of 25 kg/m^3 and thickness of 10 mm was purchased from Zhong Sheng Trade Co. (Wuyi, Zhejiang, China). Dopamine hydrochloride (98%) was obtained from J&K Scientific Ltd. (Beijing, China). Tris (hydroxymethyl) aminomethanehydrochloride (Tris-HCl) (PH 8.8, 1.5 M) was purchased from Solarbio (Beijing, China). All chemicals were used as received without further purification.

2.2. Preparation of hydrophilic PU sponge

The BPU sponges were tailored to circular with a diameter of 40 mm, and then ultrasonically washed with distilled water (DI) water and ethanol for three times, followed by drying in an oven at 50 ℃. Dopamine solution (2 mg mL^{-1}, PH=8.8) was obtained by dissolving dopamine hydrochloride in 10 mM Tris-HCl. The cleaned sponge was soaked into 20 mL freshly prepared dopamine solution followed by stirring overnight. Then, the as-prepared SM-BPU sponge was washed with DI water several times and dried in oven at 50 ℃ for 4 h.

2.3. Solar-vapor-generation experiment

The solar evaporation rates of different solar absorbers, e.g. white PU sponge, BPU sponge, and SM-BPU sponge were measured and compared with pure water, under the same solar illumination of 1 kW/m^2 over 60 min. The sponges with a diameter of 40 mm and a thickness of 10 mm were floated on top of the water surface in the beaker and exposed exactly at the center of the light beam. All sponges were twisted and soaked in DI water to be wetted before floated on the water surface. A 300W xenon lamp (PLS-SXE300; Beijing Perfect Light Technology Co., Ltd) served as the solar light source. The solar irradiation intensity of the sample surface was measured by a power meter (THORLABS, S314C). The real-time mass loss over the entire duration was recorded using a computer controlled electronic mass balance (Mettler Toledo, ME204) with accuracy of 0.1 mg. Further investigations of mass changes of water with SM-BPU

sponge under various irradiation intensities from 1 to 5 kW m^{-2} were carried out. All experiments were conducted at room temperature of 20 ±1℃ and humidity of about 60%.

2.4. Ethanol distillation

Ethanol solutions with volume fraction from 10 % to 90 % were prepared by diluting 99.8 v/v% ethanol with DI water, and charged into the beaker with diameter of 4 cm and depth of 6 cm for distillation, respectively. The beaker containing ethanol-water (70 mL) mixture and BPU sponge with a diameter of 40 mm and a thickness of 10 mm was put in a larger quartz chamber sealed by flanges. Then the beaker was irradiated under 3 kW m^{-2} of solar light. Therefore, the evaporated mixtures were condensed within the quartz chamber and the distillates were collected at the bottom of the quartz chamber. A drop of 0.3 mL distillate was used for the measurement of refractive index by using a refractive index refractometer. The mass fraction of ethanol can be converted from the refractive index by referring to a calibration standard curve of ethanol-water mixture refractive index at 20 ℃. All experiments were conducted at room temperature of 20 ±1 ℃ and humidity of around 60%.

2.5. Characterization

Field-emission scanning electron microscopy (SEM; JEOL, JEM-2100F) was performed to observe the morphologies of BPU sponge and SM-BPU sponges. The temperature of the sample was measured by an IR camera (Fluke, Model Ti400, USA) with error range of ±2 ℃. The contact angles of the sponges were obtained from a contact-angle analyzer (Ramé-hart, Inc., Model 200, USA) with accuracy of ±0.1°. A refractometer (Atago, PAL-RI, Japan) for refractive index measurement with accuracy of ±0.0003 was used to assess the ethanol concentration by measuring the refractive index at 20 ℃. An attenuated total reflection Fourier transform infrared spectroscopy (ATR-FTIR; Bruker Vertex-70, Germany) was used to verify the purity of distillate.

The spectra were obtained over a range between 400 and 4000 cm^{-1} with a spectral resolution of 4 cm^{-1}.

3. Results and discussion

3.1. Material structure and morphology

Since the fluid transport within the as-purchased BPU sponge is not good enough, it is essential to improve the hydrophilicity of the BPU sponge. It has been shown that the sponge surface modified by dopamine presents improved hydrophilicity, leading to good wettability of the sponge; in Tris-HCl aqueous solution, dopamine can spontaneously polymerize into polydopamine (PDA) with a large number of phenolic hydroxyl groups and deposit on the surface of the sponge [47, 48]. Fig. 1a shows the schematic diagram of the fabrication process. SEM observation at different magnifications was conducted to investigate the sponge surface morphology. Fig. 1b and 1c represent the SEM images of the pristine unmodified and dopamine modified BPU sponges, respectively, in different magnifications. The BPU sponge was composited with porous structure fibers with pore size of ~300 μm, and there was no obvious difference in the surface morphology of the sponges in low magnification (left column). At higher resolutions, the surface of pristine BPU sponge was quite smooth (Fig. 1b3) and the deposited PDA could be clearly observed on the skeleton of the modified sponge (Fig. 1c3), leading to a rougher surface than pristine BPU sponge.

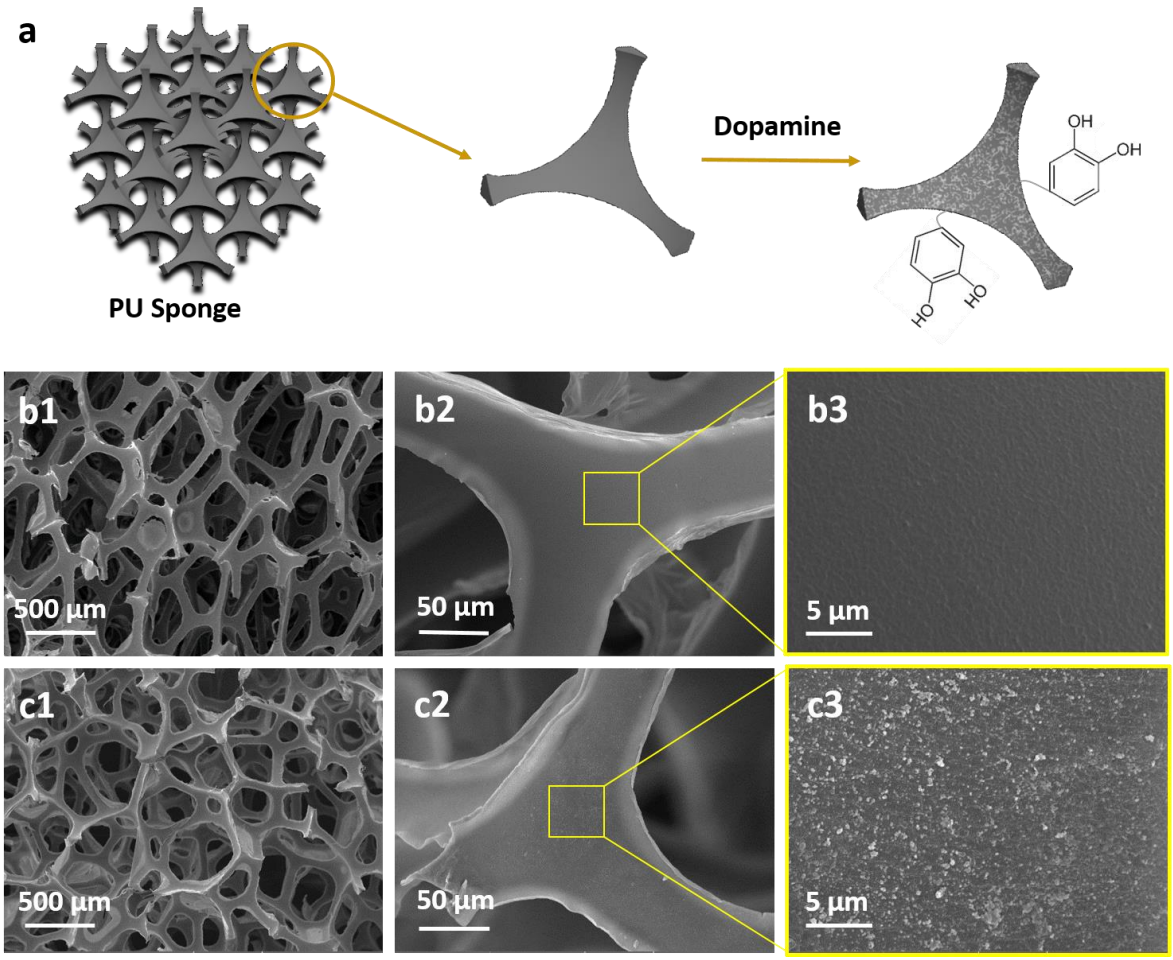

Figure 1. (a) Schematic fabrication process of SM-BPU sponge. SEM images of the BPU sponges in different magnifications: (b) pristine BPU sponge; (c) SM-BPU sponge.

The wetting property of the sponge was characterized by water contact angle measurement. After the dopamine modification, the sponge exhibited a decreased contact angle from 120° to 60°, as shown in Fig. 2a and 2b. These figures indicate the surface changing from hydrophobic into hydrophilic after the dopamine treatment. To examine the dynamics of the fluid transport in pristine and SM-BPU sponges, a 0.5 mL water droplet was added on each sponge surface to observe the water impregnation in the structure over 1s. The water quickly spread out from the touching surface in the SM-BPU sponge, while the water in the pristine sponge spread slowly as

shown on Fig. 2c. It can be concluded that the wettability was greatly promoted after dopamine modification due to the hydrophilic groups attached to the sponge surface (See Fig. 1a). The porous PU sponge has low density of 25 kg/m^3 with buoyant nature, which can float on the water surface as shown in Fig. 2d. The enhanced vapor generated by SM-BPU sponge under the solar illumination of 5 kW m^{-2} can nicely be observed.

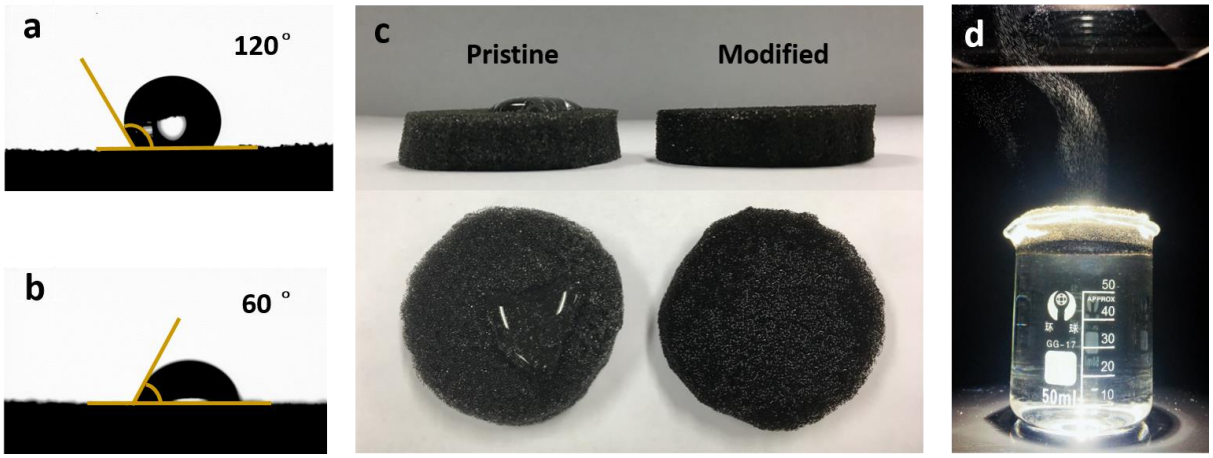

Figure 2. Contact angle measurements of (a) pristine black PU sponge and (b) dopamine modified black PU sponge. (c) Optical image to verify the dynamics of the fluid transport in pristine sponge (left) and dopamine modified sponge (right) by adding 0.5 mL water on sample surface after 1s, respectively. (d) Enhanced vapor generation by dopamine modified sponge at solar illumination of 5 kW m^{-2}.

3.2. Evaluation of the solar evaporation by PU sponges

The evaporation rates of water were recorded by measuring the mass loss as a function of time by a computer controlled electronic balance. Different experiments for measuring the evaporation rate of pure water, white PU sponge, BPU sponge, and SM-BPU sponge were respectively conducted for an hour under the same solar illumination of 1 kW m^{-2}. The exact

evaporation rates of water were recorded as shown in Fig. 3a. Water mass reductions were observed for all the experiments. Generally, the water mass loss was slow in the beginning and then became faster at a constant rate after the initial transient period. It can be explained that it takes more energy to initialize the evaporation process in the beginning. The evaporation rate of white PU sponge was as low as the natural water evaporation at about 0.23 ±0.02 kg m^{-2} h^{-1}. In comparison, with the black PU sponge, the evaporation rate was 3 times higher compared with pure water evaporation. However, the evaporation rate of the SM-BPU sponge was the highest up to 0.83 ±0.04 kg m^{-2} h^{-1}, which was 3.6 times higher than pure water under 1 kW m^{-2} solar illumination. The solar vapor generation efficiency, η_{th}, is defined as Eq. 1 [33]:

$$\eta_{\mathrm{th}} = \frac{\dot{m} h_{\mathrm{fg}}}{q_{\mathrm{solar}} A} \qquad \text{Eq. 1}$$

Where $\dot{m}$ represents the mass flux due to the evaporation, h_{fg} is the enthalpy change of liquid water to vapor phase, q_{solar} is the nominal direct solar flux per area, and A is the efficient absorber area. The evaporation efficiency was increased up to 52.2 ±2.5% by using the SM-BPU sponge. It was more than 3.5 times increment compared with the average evaporation efficiency of the pure water of 14.5%. Experiments were repeated four times under the same experimental conditions. The average values of the experimental data with error bar are presented, in which the error bar is calculated as the mean squared error of the four experimental results. The error is mainly introduced by the fluctuation of room temperature, humidity and instrument accuracy etc. The difference between each measurement is less than 5%, indicating the reproducibility of experimental data.

The evaporation efficiency of SM-BPU sponge with respect to different solar irradiation intensities were measured. Fig. 3b shows the evaporation mass loss as a function of illumination time under various solar power densities of 1 kWm^{-2}, 2 kWm^{-2}, 3 kWm^{-2}, and 5 kWm^{-2}. The

evaporation rate almost increased linearly with the solar irradiation intensity as depicted in Fig. 3c. The average evaporation rate was 0.83 kg m^{-2} h^{-1} under 1 kW m^{-2} solar illumination and it reached to 4.24 kg m^{-2} h^{-1} when the solar irradiation intensity scaled up to 5 kW m^{-2}. Fig. 3c also shows that the fluctuation of the evaporation efficiency was quite small (< 4%) as light power intensified. Clearly, this result demonstrated that the evaporation rate can be further scaled up by using optical concentrators. Figure 3d shows that similar performances of the SM-BPU sponge were achieved with mass loss of 1.03 g ±4% per hour after being used for ten cycles with 1-hour irradiation under 1 kW m^{-2} solar illumination for each cycle. These data demonstrate that the BPU sponge is durable and could be reused repeatedly without noticeable change in performance.

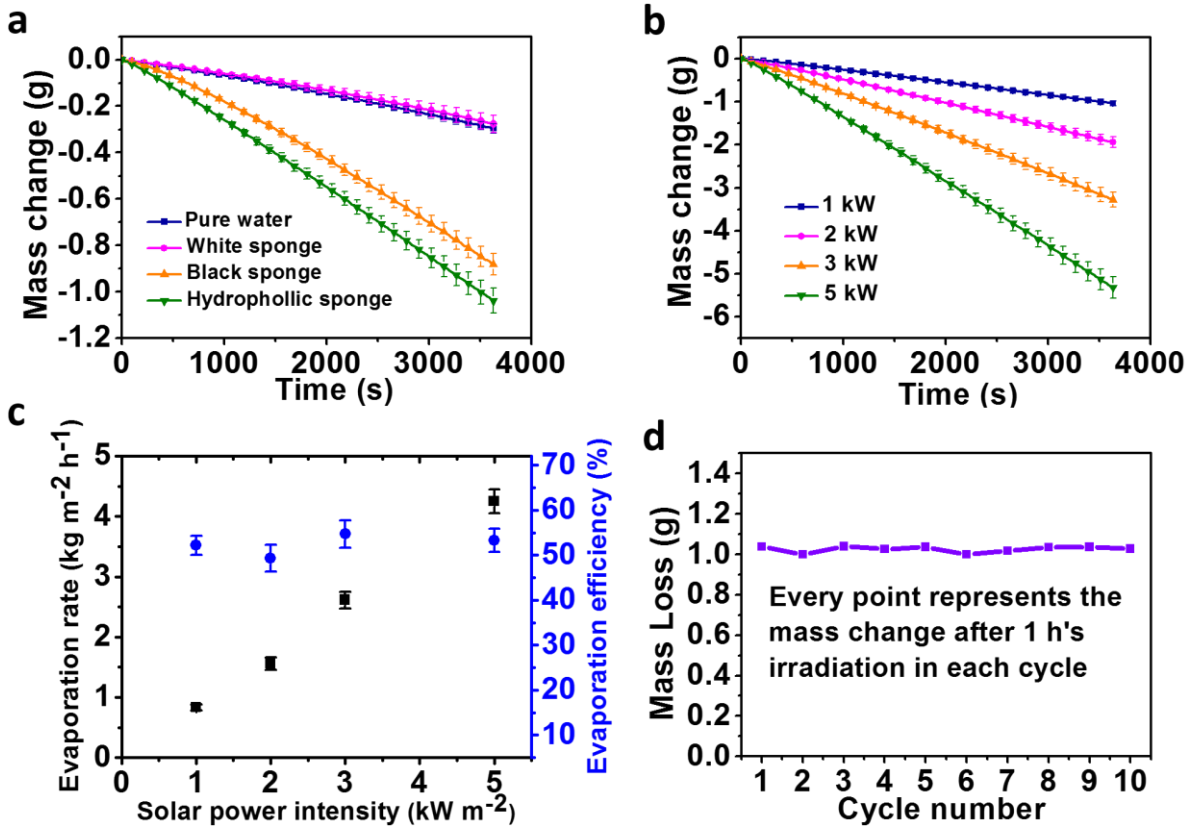

Figure 3. The solar evaporation mass loss of water over time (Each data point is an average of four measurements under the same experimental conditions): (a) with different absorbers under 1

kW m^{-2}; (b) with SM-BPU sponge under different optical densities of 1 kW m^{-2}, 2 kW m^{-2}, 3 kW m^{-2}, and 5 kW m^{-2}. (c) Corresponding evaporation rate (square) and the evaporation efficiency (circle) under different optical densities. (d) Mass loss after irradiation of the SM-BPU sponge for 10 cycles (1 hour under 1 kW m^{-2} irradiation for each cycle.).

3.3. Mechanisms of solar vapor generation enhancement

An infrared (IR) camera was utilized to determine the temperature distribution at the surface and underlying bulk water during the evaporation experiments. Before irradiation, both beakers with and without SM-BPU sponges exhibited almost the same uniform temperature distribution for the top surface and underlying water, being approximately of 21 ℃ as presented in the left columns of Fig. 4a and 4b. After the solar illumination with light density of 3 kW m^{-2} for 30 min, a remarkable difference was observed in the right columns of Fig. 4a and 4b. For the beaker without SM-BPU, the top surface temperature was 28 ℃ with only ~0.6 ℃ higher than the underlying water temperature, in which almost homogeneous temperature distribution was obtained within the beaker. However, for the beaker with SM-BPU sponge, a localized hot zone was observed only at the top surface of the water with a temperature of 56.3 ℃. In contrast, the temperature of the water below only increased up to 21.5 ℃ with the temperature difference between top and bottom of ~35 ℃. In fact, the evaporation rate of liquid is closely related to the liquid temperature, which can be evaluated by the Dalton evaporation formula: $E = C(P_s\text{-}P)$, where E, C, P_s, and P represent the evaporation rate, correlation constant, saturation vapor pressure and realistic vapor pressure of the liquid, respectively [49]. The saturation vapor pressure of water at 28 ℃ and 56.3 ℃ are 3780 and 16540 Pa, respectively, and the realistic vapor pressure of water at room temperature of 20 ℃ is about 500 Pa [50]. Based on the

calculation, after 1 h's illumination, the evaporation rate of the water on top of SM-BPU should be about 4.9 times higher than that of the control experiment with pure water only, which could account for the evaporation rate difference between them. High temperature on top of the PU sponge can be maintained because the thermal conductivity of PU sponge is low. The thermal energy diffused into the water below is resisted and therefore, heat localization is achieved at the air-water interface of the self-floating SM-BPU sponge. Besides, after one-step dopamine treatment, the hydrophilic property of the BPU has been improved because water can be more effectively transported into the air-water interface through the porous transport channels and conveyed into vapor phase. This also explains why the evaporation efficiency can be further enhanced through dopamine treatment. These are the reasons making SM-BPU sponge based solar evaporation an efficient process.

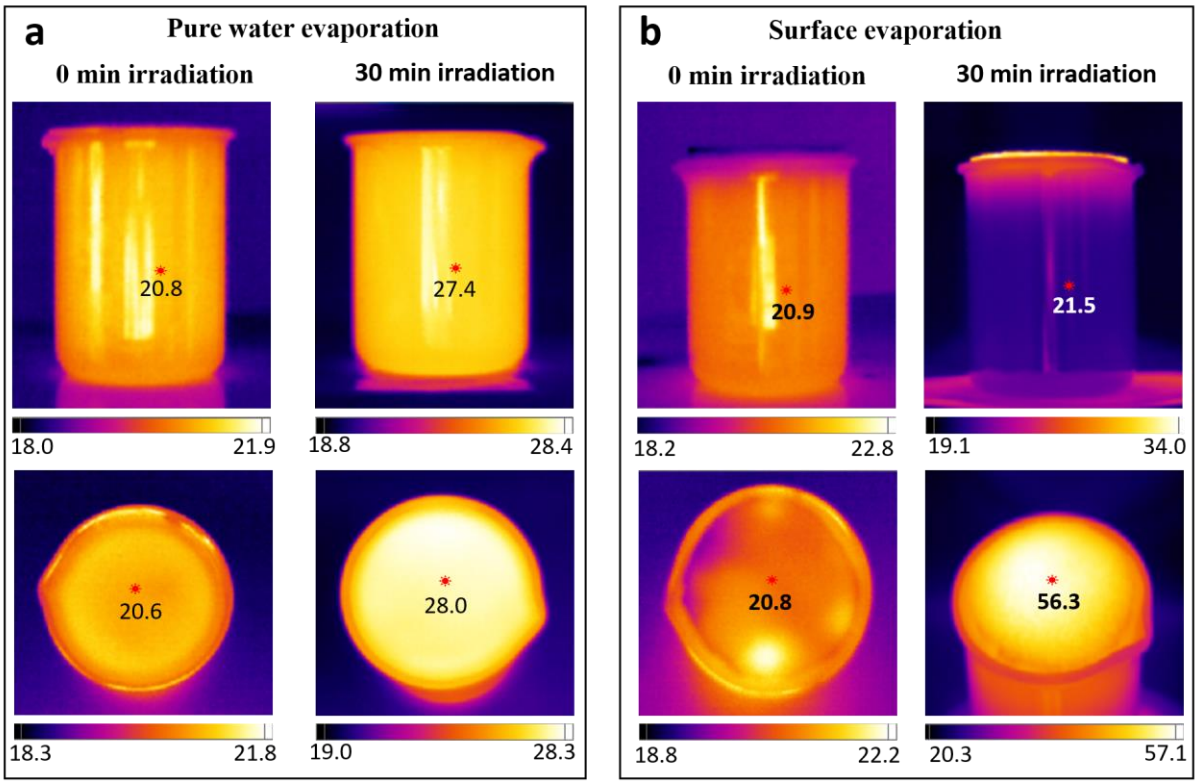

Figure 4. Side view and top view images of temperature distribution by IR camera: (a) pure

water evaporation at 0 min irradiation and at 30 min irradiation; (b) surface evaporation with free-floating dopamine modified sponge at 0 min irradiation and 30 min irradiation. The optical intensity was set to be 3 kW m^{-2}.

3.4. Ethanol distillation and potential applications

Distillation, which can be used to separate liquids with different boiling points, is the most dominant industrial purification technique for ethanol production. Here, we examined the performance of the BPU sponge for distilling the ethanol-water mixtures. Fig. 5a shows the photo of the solar ethanol distillation experimental set up. A beaker containing ethanol-water mixtures (70 mL) with self-floating BPU sponge was put inside a larger sealed quartz chamber. The distillate was collected at the bottom of this larger quartz chamber, and then analyzed by a refractometer for the fraction of the ethanol within the sample fluid. The vapor-liquid diagram of ethanol-water mass fraction was obtained based on the measured refractive index of distillates, as shown in Fig. 5b. A black dot line representing an equal concentration of ethanol for both the liquid and vapor state was drawn for clearly displaying the improvement of ethanol concentration. Fig. 5 b shows that the lower liquid mass fraction of ethanol (< 0.6 (60 wt%)) mixture was distilled to much higher ethanol mass fraction (with maximum up to 25 wt% increment) for each distillation cycle by using the BPU sponge. No further ethanol mass fraction enhancement was observed for the liquid mass fraction of ethanol beyond 0.6 (60 wt %). The highest mass fraction of ethanol of the distillate is about 70 ±0.02 wt%, which was achieved from distilling higher mass fraction of ethanol liquid of 0.9 (90 wt %). It could be due to high humidity level in the ambient air in Hong Kong. Because of the hygroscopic nature of ethanol, it absorbed water vapor directly from the atmosphere, leading to saturation of further ethanol

enhancement. For this reason, it is quite likely that higher ethanol concentration can be obtained with this black PU sponge through humidity control. Besides, ATR-FTIR was applied to study the chemical structures of liquid samples before and after the distillation to verify if there was any new structure being introduced after distillation. As presented in Fig. 5c, both spectra show the same absorption peaks with an OH stretch, a CH stretch, CO stretches and various bending vibrations, which are consistent with those of standard ethanol liquid [51, 52]. It indicates that no new chemical structures were added into the distillate, which reflects that volatile organic contaminants were not likely to be found in distillate. Therefore, this first demonstration confirmed that BPU sponge can be used for solar ethanol concentration enrichment. The application of ethanol as a fuel is necessary to reach a concentration of 95 wt% [53]. Certainly, solar energy can take a part in the preliminary concentration process of ethanol freshly produced from fermentation with initial concentration of ~10 wt%, then followed by additional process such as industrial heat distillation to obtain the concentration greater than 95 wt%, which can surely greatly reduce the amount of fossil energy needed for the fuel grade ethanol production.

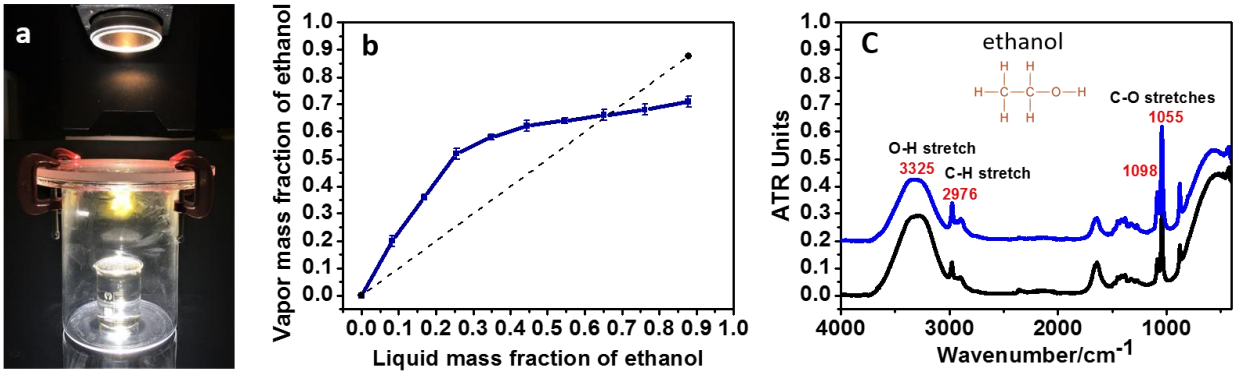

Figure 5. (a) Picture of the solar distillation setup; (b) vapor-liquid diagram of the ethanol-water mass fraction obtained by solar distillation (Each data point is an average of four measurements under the same experimental conditions). The black dot line represents an equal mass fraction of ethanol in both liquid and vapor state. (c) ATR-FTIR spectra (absorbance mode) of pristine 40

v/v% ethanol-water mixture (black curve) and corresponding distillate (blue curve).

Moreover, solar fresh water generation from sea/waste water can be achieved by constructing a complete system with continuous sea/waste water supply and evaporation water collection. The average evaporation rate achieved in this experiment was 0.83 kg m^{-2} h^{-1} under 1 kW m^{-2} solar illumination. Assuming only 0.5 L m^{-2} h^{-1} water (60% of achieved efficiency in lab) can be collected from the system, average sunlight hours per day is 5.22 hours (average in Hong Kong) and only 20 liters of water per adult per day are required. For a typical village house in Hong Kong with roof top area of 65 m^2, the quantity of water generated on average per day is around (65×5.22×0.5) 169 liters, which can meet the basic food and hygiene needs of about 8 adults. Therefore, utilization of the BPU sponges as solar absorber materials shows promising prospect in practical applications.

4. Conclusions

In this study, we have successfully demonstrated significant efficiency enhancement for solar vapor generation by using the recycled waste BPU sponge and solar energy. Via one-step treatment of dopamine solution, the wettability of the black PU sponge was improved for fast dynamics of the fluid transport within the sponge. The porous floatable BPU sponge with low thermal conductivity and high durability generated localized heat at the air-water surface so as to effectively enhance the water evaporation efficiency. The solar vapor generation efficiency reached 52.2 ±2.5% by using the proposed SM-BPU solar absorber, which was more than 3.5 times higher than the natural evaporation process (14.5%). The BPU sponge was also examined for application in ethanol distillation. The results show that the low mass fraction of ethanol

mixture could be distilled to a higher mass fraction (up to 25 wt% concentration improvement for each distillation cycle). Remarkably, the recycling of the waste BPU sponge into useful and efficient solar absorber materials for vapor generation can reduce environmental pressure, which is more competitive compared with conventional evaporation systems. Such technology can be further developed into a system with continues sea/waste water supply and evaporated water collection for generation of fresh water from sea/waste water in those areas with very limited fresh water supply, e.g. island. It also can be used for chemical distillation, e.g. alcohol concentration for biofuel production, to reduce the cost of distillation.

Acknowledgments

This work is financially supported by the National Natural Science Foundation of China (Grant No. 61575167), the Research Grants Council of Hong Kong, China (Project Number: GRF 152109/16E PolyU B-Q52T), and the Hong Kong Polytechnic university (Project Number: 1-ZVGH, G-UA7N).

References

[1] Lewis NS, Nocera DG. Powering the planet: Chemical challenges in solar energy utilization. Proc Natl Acad Sci USA 2006;103:15729-35.
[2] Yang J, Pang Y, Huang W, Shaw SK, Schiffbauer J, Pillers MA, et al. Functionalized graphene enables highly efficient solar thermal steam generation. ACS Nano 2017;11:5510-18.
[3] Grätzel M. Photoelectrochemical cells. Nature 2001;414:338-44.
[4] Kamat PV. Meeting the clean energy demand: nanostructure architectures for solar energy conversion. J Phys Chem C 2007;111:2834-60.
[5] Walter MG, Warren EL, McKone JR, Boettcher SW, Mi Q, Santori EA, et al. Solar water splitting cells. Chem Rev 2010;110:6446-73.
[6] Wu XD, Xia XH, Chen GQ, Wu XF, Chen B. Embodied energy analysis for coal-based power generation system-highlighting the role of indirect energy cost. Appl Energy 2016;184:936-50.
[7] Yue T, Lior N. Exergo economic analysis of solar-assisted hybrid power generation systems integrated with thermochemical fuel conversion. Appl Energy 2017;191:204-22.

[8] Abraham J, Plourde B, Minkowycz W. Continuous flow solar thermal pasteurization of drinking water: methods, devices, microbiology, and analysis. Renew Energy 2015;81:795-803.
[9] Mehr AS, Gandiglio M, MosayebNezhad M, Lanzini A, Mahmoudi SMS, Yari M, et al. Solar-assisted integrated biogas solid oxide fuel cell (SOFC) installation in wastewater treatment plant: energy and economic analysis. Appl Energy 2017;191:620-38.
[10] Rizzo L, Della Sala A, Fiorentino A, Puma GL. Disinfection of urban wastewater by solar driven and UV lamp-TiO_2 photocatalysis: effect on a multi drug resistant Escherichia coli strain. Water Res 2014;53:145-52.
[11] Hamed OA, Kosaka H, Bamardouf KH, Al-Shail K, Al-Ghamdi AS. Concentrating solar power for seawater thermal desalination. Desalination 2016;396:70-8.
[12] Li G-P, Zhang L-Z. Investigation of a solar energy driven and hollow fiber membrane-based humidification-dehumidification desalination system. Appl Energy 2016;177:393-408.
[13] Suárez F, Ruskowitz JA, Tyler SW, Childress AE. Renewable water: direct contact membrane distillation coupled with solar ponds. Appl Energy 2015;158:532-9.
[14] Neumann O, Urban AS, Day J, Lal S, Nordlander P, Halas NJ. Solar vapor generation enabled by nanoparticles. ACS Nano 2012;7:42-9.
[15] Neumann O, Neumann AD, Silva E, Ayala-Orozco C, Tian S, Nordlander P, et al. Nanoparticle-mediated, light-induced phase separations. Nano lett 2015;15:7880-5.
[16] Hogan NJ, Urban AS, Ayala-Orozco C, Pimpinelli A, Nordlander P, Halas NJ. Nanoparticles heat through light localization. Nano Lett 2014;14:4640-5.
[17] Wang Z, Liu Y, Tao P, Shen Q, Yi N, Zhang F, et al. Bio-inspired evaporation through plasmonic film of nanoparticles at the air-water interface. Small 2014;10:3234-9.
[18] Zhou L, Tan Y, Wang J, Xu W, Yuan Y, Cai W, et al. 3D self-assembly of aluminium nanoparticles for plasmon-enhanced solar desalination. Nat Photonics 2016;10:393-8.
[19] Liu Y, Yu S, Feng R, Bernard A, Liu Y, Zhang Y, et al. A bioinspired, reusable, paper-based system for high-performance large-scale evaporation. Adv Mater 2015;27:2768-74.
[20] Zhou L, Tan Y, Ji D, Zhu B, Zhang P, Xu J, et al. Self-assembly of highly efficient, broadband plasmonic absorbers for solar steam generation. Sci Adv 2016;2:e1501227.
[21] Liu C, Huang J, Hsiung CE, Tian Y, Wang J, Han Y, et al. High-performance large-scale solar steam generation with nanolayers of reusable biomimetic nanoparticles. Adv Sustain Syst 2017;1:1600013.
[22] Wang X, He Y, Liu X, Cheng G, Zhu J. Solar steam generation through bio-inspired interface heating of broadband-absorbing plasmonic membranes. Appl Energy 2017;195:414-25.
[23] Zedan AF, Moussa S, Terner J, Atkinson G, El-Shall MS. Ultrasmall gold nanoparticles anchored to graphene and enhanced photothermal effects by laser irradiation of gold nanostructures in graphene oxide solutions. ACS Nano 2012;7:627-36.
[24] Liu Y, Chen J, Guo D, Cao M, Jiang L. Floatable, self-cleaning, and carbon-black-based superhydrophobic gauze for the solar evaporation enhancement at the air-water interface. ACS Appl Mater Inter 2015;7:13645-52.
[25] Liu Z, Song H, Ji D, Li C, Cheney A, Liu Y, et al. Extremely cost-effective and efficient solar vapor generation under nonconcentrated illumination using thermally isolated black paper. Global Challenges 2017;1: 1600003.
[26] Wang Y, Zhang L, Wang P. Self-floating carbon nanotube membrane on macroporous silica substrate for highly efficient solar-driven interfacial water evaporation. ACS Sustain Chem Eng 2016;4:1223-30.
[27] Ito Y, Tanabe Y, Han J, Fujita T, Tanigaki K, Chen M. Multifunctional porous graphene for

high-efficiency steam generation by heat localization. Adv Mater 2015;27:4302-7.
[28] Hu X, Xu W, Zhou L, Tan Y, Wang Y, Zhu S, et al. Tailoring graphene oxide-based aerogels for efficient solar steam generation under one sun. Adv Mater 2017;29:1604031.
[29] Zhang L, Tang B, Wu J, Li R, Wang P. Hydrophobic light-to-heat conversion membranes with self-healing ability for interfacial solar heating. Adv Mater 2015;27:4889-94.
[30] Liu K-K, Jiang Q, Tadepalli S, Raliya R, Biswas P, Naik RR, et al. Wood-graphene oxide composite for highly efficient solar steam generation and desalination. ACS Appl Mater Inter 2017;9:7675-81.
[31] Xue G, Liu K, Chen Q, Yang P, Li J, Ding T, et al. Robust and low-cost flame-treated wood for high-performance solar steam generation. ACS Appl Mater Inter 2017;9:15052-7.
[32] Xu N, Hu X, Xu W, Li X, Zhou L, Zhu S, et al. Mushrooms as efficient solar steam-generation devices. Adv Mater 2017;1606762.
[33] Ghasemi H, Ni G, Marconnet AM, Loomis J, Yerci S, Miljkovic N, et al. Solar steam generation by heat localization. Nat Commun 2014;5:4449.
[34] Wang G, Fu Y, Ma X, Pi W, Liu D, Wang X. Reusable reduced graphene oxide based double-layer system modified by polyethylenimine for solar steam generation. Carbon 2017;114:117-24.
[35] Jiang Q, Tian L, Liu KK, Tadepalli S, Raliya R, Biswas P, et al. Bilayered biofoam for highly efficient solar steam generation. Adv Mater 2016;28:9400-7.
[36] Ni G, Li G, Boriskina SV, Li H, Yang W, Zhang T, et al. Steam generation under one sun enabled by a floating structure with thermal concentration. Nat Energy 2016;1:16126.
[37] Polyurethane, the Essential Chemical Industry, 2013; http://www.essentialchemicalindustry.org/polymers/polyurethane.html.
[38] New forecasts for polypropylene, polystyrene and polyurethane, Gobi International, May 20, 2002; http://www. gobi.co.uk/press/PolyPress2002.pdf.
[39] Usman M, Adeosun S, Osifeso G. Optimum calcium carbonate filler concentration for flexible polyurethane foam composite. JOM 2012;11:311.
[40] Howard GT. Biodegradation of polyurethane: a review. Int Biodeter Biodegr 2002;49:245-52.
[41] Zia KM, Bhatti HN, Bhatti IA. Methods for polyurethane and polyurethane composites, recycling and recovery: a review. React Funct Polym 2007;67:675-92.
[42] Zhang X, Li Z, Liu K, Jiang L. Bioinspired multifunctional foam with self-cleaning and oil/water separation. Adv Funct Mater 2013;23:2881-6.
[43] Liu Y, Ma J, Wu T, Wang X, Huang G, Liu Y, et al. Cost-effective reduced graphene oxide-coated polyurethane sponge as a highly efficient and reusable oil-absorbent. ACS Appl Mater Inter 2013;5:10018-26.
[44] Pu X, Liu X, Qiu F, Huang L. Novel method to optimize the structure of reticulated porous ceramics. J Am Ceram Soc 2004;87:1392-4.
[45] Alvarez S, Fuertes AB. Synthesis of macro/mesoporous silica and carbon monoliths by using a commercial polyurethane foam as sacrificial template. Mater Lett 2007;61:2378-81.
[46] Wu J-W, Sung W-F, Chu H-S. Thermal conductivity of polyurethane foams. Int J Heat Mass Tran 1999;42:2211-7.
[47] Li B, Li L, Wu L, Zhang J, Wang A. Durable superhydrophobic/superoleophilic polyurethane sponges inspired by mussel and lotus leaf for the selective removal of organic pollutants from water. ChemPlusChem 2014;79:850-6.
[48] Wang H, Wang E, Liu Z, Gao D, Yuan R, Sun L, et al. A novel carbon nanotubes reinforced

superhydrophobic and superoleophilic polyurethane sponge for selective oil-water separation through a chemical fabrication. J Mater Chem A 2015;3:266-73.
[49] Sartori E. A critical review on equations employed for the calculation of the evaporation rate from free water surfaces. Sol Energy 2000;68:77-89.
[50] Wexler A. Vapor pressure formulation for water in range 0 to 100 C. A revision. J Res Natl Bur Stand A 1976;80:775-85.
[51] Doroshenko I, Pogorelov V, Sablinskas V. Infrared absorption spectra of monohydric alcohols. Dataset Pap Chem 2013;6: 329406.
[52] Corsetti S, Zehentbauer FM, McGloin D, Kiefer J. Characterization of gasoline/ethanol blends by infrared and excess infrared spectroscopy. Fuel 2015;141:136-42.
[53] Vargas-Bautista JP, García-Cuéllar AJ, Pérez-García SL, Rivera-Solorio CI. Transient simulation of a solar heating system for a small-scale ethanol-water distillation plant: thermal, environmental and economic performance. Energy Convers Manage 2017;134:347-60.